Human Molecular Genetics, 2014, Vol. 23, No. 23 **6318–6331**
doi:10.1093/hmg/ddu350
Advance Access published on July 4, 2014

SMN regulates axonal local translation via miR-183/mTOR pathway

Min Jeong Kye[1,2], Emily D. Niederst[1], Mary H. Wertz[1], Inês do Carmo G. Gonçalves[2], Bikem Akten[1], Katarzyna Z. Dover[4,5], Miriam Peters[2,3], Markus Riessland[2,3], Pierre Neveu[7,8,9], Brunhilde Wirth[2,3], Kenneth S. Kosik[8], S. Pablo Sardi[10], Umrao R. Monani[4,5,6], Marco A. Passini[10] and Mustafa Sahin[1,*]

[1]Department of Neurology, The F. M. Kirby Neurobiology Center, Boston Children's Hospital, Harvard Medical School, Boston, MA, USA, [2]Institute of Human Genetics, Institute for Genetics and, [3]Center of Molecular Medicine Cologne, University of Cologne, Cologne, Germany, [4]Center for Motor Neuron Biology and Disease, [5]Department of Pathology and Cell Biology and, [6]Department of Neurology, Columbia University Medical Center, New York, NY 10032, USA, [7]Kavli Institute for Theoretical Physics and, [8]Neuroscience Research Institute, University of California at Santa Barbara, Santa Barbara, CA 93106, USA, [9]Cell Biology and Biophysics Unit, European Molecular Biology Laboratory, 69117, Heidelberg, Germany and [10]Genzyme, a Sanofi Company, Framingham, MA 01701, USA

Received April 18, 2014; Revised June 27, 2014; Accepted July 2, 2014

Reduced expression of SMN protein causes spinal muscular atrophy (SMA), a neurodegenerative disorder leading to motor neuron dysfunction and loss. However, the molecular mechanisms by which SMN regulates neuronal dysfunction are not fully understood. Here, we report that reduced SMN protein level alters miRNA expression and distribution in neurons. In particular, miR-183 levels are increased in neurites of SMN-deficient neurons. We demonstrate that miR-183 regulates translation of *mTor* via direct binding to its 3′ UTR. Interestingly, local axonal translation of *mTor* is reduced in SMN-deficient neurons, and this can be recovered by miR-183 inhibition. Finally, inhibition of miR-183 expression in the spinal cord of an SMA mouse model prolongs survival and improves motor function of *Smn*-mutant mice. Together, these observations suggest that axonal miRNAs and the mTOR pathway are previously unidentified molecular mechanisms contributing to SMA pathology.

INTRODUCTION

MicroRNAs are molecular regulators of protein expression that act by repressing translation or destabilizing mRNAs. Numerous miRNAs have been described in many organisms and are reported to play significant roles in a broad range of cellular and developmental processes, including cell cycle (1), neuronal development (2) and learning and memory (3,4). RISC (RNA-induced silencing complex) is a ribonucleoprotein complex comprised of targeting miRNAs and a number of associated proteins including Argonautes and GW182 proteins (5). Proteins involved in miRNA function have been detected in axons of primary hippocampal and sympathetic neurons (6–8). Furthermore, Mov10, a component of the RISC complex, is also present at mammalian synaptic sites, where it regulates protein translation in response to neuronal activity (9). These findings strongly suggest that miRNAs act as important regulators of local axonal protein translation in neurons (10).

Deficiency of SMN leads to spinal muscular atrophy (SMA), an autosomal recessive disease characterized by spinal motor neuron degeneration (11,12). Spinal muscular atrophy is caused by homozygous deletion or mutation of *SMN1* (*survival motor neuron 1*). *SMN2*, which is >99% identical to *SMN1*, contains a single nucleotide change that produces aberrant splicing lacking exon 7. Therefore, only ∼10% of *SMN2* transcripts are properly spliced and synthesize functional full-length SMN proteins. *SMN2* can vary from 1 to 6 copies per genome and is the main modifier of SMA to influence SMA severity (11). SMN protein is ubiquitously expressed in all neuronal compartments including the nucleus, soma, axon and dendrites (13,14). Within the nucleus, SMN is localized in subcellular structures called gems, where it interacts with a number of proteins essential

*To whom correspondence should be addressed at: F. M. Kirby Neurobiology Center, Children's Hospital, 300 Longwood Avenue CLSB 14073, Boston, MA 02115, USA. Tel: +1 6179194518; Fax: +1 6177300242; Email: mustafa.sahin@childrens.harvard.edu

to RNA processing and splicing including the Gemin3 and Gemin4 proteins, which can also be found in the RISC complex (15–18). In the axons and dendrites of neurons, SMN interacts with RNA-binding proteins, such as HuD, and plays a role in ribonucleoprotein (RNP) trafficking required to accomplish local protein translation in these compartments (14,19,20). SMN also binds FMRP (21) and KSRP (22), which are important for miRNA biogenesis and function (23). Recently, it was reported that mice lacking the miRNA-processing enzyme Dicer selectively in motor neurons display SMA-like phenotype, arguing for a potential role for miRNAs in neuromuscular disorders (24).

Local axonal protein translation has also been implicated in SMA pathology (25,26). Interestingly, when full-length SMN level is reduced, axons are shorter and growth cones are smaller (27). The most extensively investigated mRNA that undergoes local translation in axonal growth cones is *β-actin,* which may contribute to the observed deficits in axonal actin cytoskeleton organization found in SMA animal models (27). Recently, we reported *cpg15* (neuritin) mRNA found in axons is regulated locally by SMN and HuD (14). These results indicated that SMN could regulate the expression/trafficking of a number of mRNAs locally translated in neurites. Given that SMN binds to KSRP (22) and FMRP (21), we hypothesized that SMN complex plays a role in the regulation of miRNA expression and within neurons to regulate local translation.

Here, we demonstrate that reduced SMN levels triggered differential expression and distribution of specific miRNAs in neurons. Among the miRNAs up-regulated in SMN-deficient neurons, miR-183 can suppress axon growth. We show that miR-183 regulated translation of *mTor* mRNA via direct binding to its 3′ UTR, providing a novel link between SMN deficiency and a miRNA-mediated regulation of a key growth and survival pathway. Furthermore, we are able to demonstrate modest prolongation of survival and improved motor function *in vivo*, in the setting of an animal model for SMA by inhibiting the elevated miR-183 expression selectively in spinal motor neurons. These findings shed light on previously unidentified mechanisms implicated in SMA pathology and provide new insight into the contribution of miRNA dysregulation to the pathology of neurological disorders.

RESULTS

Reduced SMN level alters miRNA expression and distribution in neurons

To examine levels of miRNA expression in neurites, we cultured embryonic rat cortical neurons in modified Boyden chambers (14,28). These chambers allow separation of neurites (axons and dendrites) from cell bodies and produce a substantial quantity of RNAs for consistent profiling of miRNA expression (Supplementary Material, Fig. S1A). After 10 days *in vitro* (DIV), total protein and RNA were extracted from the upper chamber, which contains mainly the cell body compartment and from the lower chamber, which contains the distal neurites. We confirmed the separation of the cellular compartments by measuring Tau protein, which is enriched in distal axons, and Lamin A, a marker of the nuclear envelope (Supplementary Material, Fig. S1B). Integrity of RNA samples was confirmed by measuring known mRNA expression (29). The best-characterized mRNA in the axon, *β-actin*, was expressed at similar levels in the cell body and neurite samples. In contrast, *γ-actin* mRNA and snoRNA U6B were detected at a much lower level in the neurites, as compared with the cell body compartment (Supplementary Material, Fig. S1C and D), as previously described (29).

To test whether SMN plays a role in miRNA expression and distribution in neurons, we knocked down SMN expression using lentivirus expressing shRNA against rat *Smn*. Nine days after infection, *Smn* mRNA is reduced to ∼45% of control in the cell body compartment and to <25% of control in the neurite compartment (Supplementary Material, Fig. S1E). We also confirmed that SMN protein is reduced to ∼40% of control (Supplementary Material, Fig. S1F). Using these RNA samples, we measured the expression of 187 miRNAs with Taqman-based multiplexed real-time PCR. Most miRNAs measured could be detected in the neurite compartment and showed differential distributions between cell bodies and neurites (Supplementary Material, Fig. S1G and Table S1). This finding is consistent with previous reports that used laser capture microdissection of neurites from hippocampal neurons (7) and axonal miRNA profiling in sympathetic neurons (8). We then compared the expression and distribution of miRNAs in control and *Smn*-knockdown neurons (Supplementary Material, Fig. S1G and Tables S2–S5). While the overall distribution of miRNAs was not significantly affected (Supplementary Material, Fig. S1H), there were differences in the distribution of individual miRNAs (Supplementary Material, Tables S2–S5). Because complete SMN depletion in neuronal cells can cause cell death (30), we measured levels of caspase activity in *Smn*-knockdown neurons and confirmed that the apoptosis pathways were not yet active in our samples at the time of RNA collection (Supplementary Material, Fig. S1I). Furthermore, there was no increase in RIP1 expression as a marker of necrosis (31) after *Smn*-knockdown (Supplementary Material, Fig. S1J). Thus, alterations in miRNA expression observed in SMN-deficient neurons are not due to cell death.

Because we are particularly interested in miRNA function in the neurites, we focused on miRNAs whose expression is primarily changed in the neurite samples but not in cell body samples of *Smn*-knockdown neurons. Thus, miRNAs such as miR-30a-5p and miR-196b, whose expressions were altered in both cell body and neurites samples of *Smn*-knockdown neurons, were excluded from further investigation. In control neurons, miR-183 is expressed at higher levels in the cell body than in the neurites. Upon Smn-knockdown, its expression increases two-fold in the neurite compartment without a significant change in the cell body compartment (Fig. 1A, Supplementary Material, Tables S2 and S4). Thus, we selected miR-183 to characterize further. Overall expression of miR-183 in the whole cell was increased in both spinal motor and cortical neuron cultures following *Smn*-knockdown (Fig. 1B, Supplementary Material, Fig. S2A and B). We also found that miR-183 expression was elevated in SMA type 1 patient-derived fibroblast cell lines, as well as spinal cord and sciatic nerve from 4-day-old SMA model mice (FVB, $Smn^{-/-}$;$SMN2^{tg/tg}$;$SMN\Delta7^{tg/tg}$) (Fig. 1C–E, Supplementary Material, Table S6). The sciatic nerve is made up of axons from sensory and motor neurons; therefore, these data support our finding that miR-183 expression is increased in the neurite compartment. As a control, we measured the expression of other miRNAs in our samples such as miR-124a,

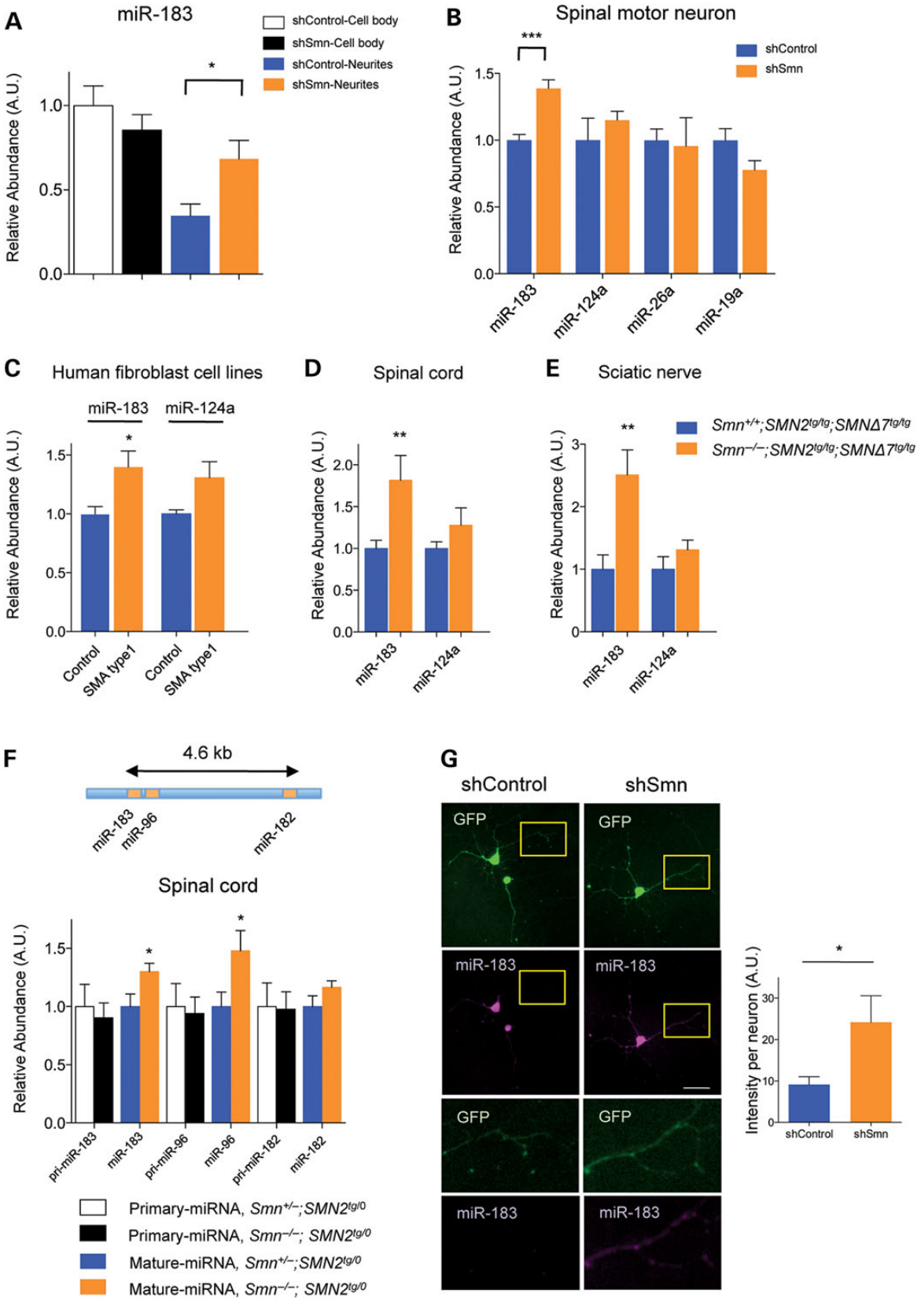

Figure 1. Expression and distribution of miR-183 is altered in SMN-deficient cells. (**A**) Real-time PCR of miR-183 expression in subcellular compartment of control and *Smn*-knockdown cortical neurons. $n = 8$ from four different biological samples. (**B**) Real-time PCR showing miR-183 expression in *Smn*-knockdown spinal motor neurons. Spinal motor neurons were isolated from E15 rat embryos and cultured 7 days. $n = 6$ from three biological samples. (**C**) Real-time PCR showing miR-183

miR-19a and miR-26a, and these did not change with SMN loss (Fig. 1B–E). Another SMA mouse model, which contains two copies of *SMN2* per integrate in their genome [FVB, $Smn^{-/-}$;$SMN2^{tg/0}$ (32)], also displayed higher level of miR-183 expression in the spinal cord (Fig. 1F). Together, these data indicate that reduced neuronal SMN level increases miR-183 expression.

To explore the cellular mechanism of elevated miR-183 expression, we measured the primary transcript of miR-183 in P4 spinal cord of the SMA mouse model containing two copies of human *SMN2* (FVB, $Smn^{-/-}$;$SMN2^{tg/0}$). Because miR-183 is transcribed as a single transcript together with miR-96 and miR-182, we also measured expression of the other two miRNAs in the same gene cluster (Fig. 1F). Interestingly, the amount of primary transcript was not increased in the spinal cord of SMA mouse model, whereas expression of the mature forms of miR-183 and miR-96 was increased. In contrast, another miRNA in the cluster, miR-182, was unchanged. These data suggest that there is differential regulation of biogenesis among miRNAs in the miR-183∼96∼182 cluster and that reduced SMN level causes dysregulation in the miRNA biogenesis pathway, rather than in overall transcription.

To confirm the up-regulation of miR-183 in the neurites, we performed *in situ* hybridization in rat hippocampal and spinal motor neurons. *Smn*-knockdown neurons displayed higher expression of miR-183 throughout their neurites. miR-183 levels in the neurite, normalized to those in the cell body of individual neurons, confirmed our real-time PCR data that miR-183 expression is elevated two-fold in the neurites of SMN-deficient neurons (Fig. 1G and Supplementary Material, Fig. S2C). Using real-time PCR, miR-183 was detectable in hippocampal, cortical and spinal motor neuron cultures, but it was detected at lower levels in the spinal motor neurons (Supplementary Material, Fig. S2D). Taken together, these results indicate that SMN deficiency elevates expression of miR-183 in several types of cells and tissues.

Inhibition of miR-183 rescues the Smn-knockdown axonal phenotype in neurons

As miR-183 expression is up-regulated in SMN-deficient neurons, we asked whether reducing miR-183 levels could rescue the impaired axonal growth seen in rat *Smn*-knockdown neurons (Fig. 2A–G). We adapted siRNA technology to knockdown *Smn* expression more rapidly than lentiviral shRNA because axonal morphology must be measured when axons are shorter, at 5 DIV. Forty-eight hours after siRNA transfection, expression of *Smn* mRNA was reduced to ∼50% of initial levels and protein to <10% of the control, using two different siRNAs against *Smn* (Fig. 2B and Supplementary Material, Fig. S3A). We simultaneously reduced the expression of miR-183 to <10% using locked nucleic acid (LNA) inhibitor, a DNA oligonucleotide with reverse complementary sequence of miR-183 (Fig. 2C). After 48 h of transfection, we visualized transfected LNA oligonucleotide with FITC-conjugated streptavidin and found that >90% of neurons were transfected with LNA inhibitor (Supplementary Material, Fig. S3B). Inhibition of miR-183 lasts about 10 days whereas miR-183 expression increases gradually as the neurons mature in culture (Supplementary Material, Fig. S3C and D). Interestingly, miR-183 knockdown rescued the impairment of axonal growth in *Smn*-knockdown neurons. Both the longest and total axon lengths were comparable with controls in *Smn*-knockdown neurons transfected with miR-183 LNA inhibitor (Fig. 2A, D and E). The miR-183 LNA inhibitor, however, increased the number of branches and percentage of neurons with multiple axons to above the control levels (Fig. 2F and G). Taken together, these findings suggest that reduction of miR-183 partially compensates for SMN deficiency in neurons.

miR-183 regulates mTOR activity by directly binding to the 3′ UTR of mTor

To understand how miR-183 knockdown affects neurons, we first used a computational approach using miRanda to find downstream target genes of miR-183. A previous study indicates that miR-183 cluster regulates the PI3K/AKT/mTOR pathway in medulloblastoma cell lines (33). As we had previously demonstrated that mTOR hyperactivity results in aberrant neuronal growth and multiple axons (34), similar to what we observe with miR-183 knockdown, we specifically searched for genes in this pathway among putative target genes (387 genes for rat and 717 genes for mouse are predicted targets of miR-183). As *mTor* mRNA itself contains putative binding sequence for miR-183 (Fig. 3A), we asked whether *mTor* is *bona fide* target of miR-183. We over-expressed miR-183 using pre-miR-183 and inhibited miR-183 using LNA inhibitor in neurons and then measured protein and mRNA levels of putative target genes. Up- or down-regulating miR-183 expression significantly changed the protein levels of *mTor* without altering its mRNA level (Fig. 3B, C and Supplementary Material, Fig. S4). These findings indicate that miR-183 regulates protein expression of *mTor* at the post-transcriptional level.

To determine whether miR-183 regulates the mRNA translation of *mTor* directly, we constructed a reporter system expressing firefly luciferase fused to the 3′ UTR of this gene (Fig. 3D). We measured the firefly luciferase activity with gain- or loss- of miR-183 function in HEK293T cells. Inhibition of miR-183 increased firefly luciferase activity of the reporter construct whereas overexpression of miR-183 reduced its expression. *mTor* 3′ UTR has only one putative binding site for miR-183, and mutation of six nucleotides in seed region of this site abolished

expression in type 1 SMA patient-derived fibroblast cell lines. A control and two type I SMA cell lines were analyzed, and each cell line was examined at two different passages except for the control cell line. Genetic and clinical information about the cell lines are in Supplementary Material, Table S6. (**D, E**) miR-183 expression in spinal cord (**D**) and sciatic nerve (**E**) of postnatal day 4 (P4) SMA mice. $n = 5$ for control ($Smn^{+/+}$;$SMN2^{tg/tg}$;$SMN\Delta7^{tg/tg}$) and $n = 7$ for SMA animals ($Smn^{-/-}$; $SMN2^{tg/tg}$; $SMN\Delta7^{tg/tg}$). (**F**) Schematic representation of miR-183∼96∼182 cluster in the mouse genome. Real-time PCR of primary transcript and mature form of miRNAs from this cluster were measured in the spinal cord of P4 SMA mice. $n = 9$ for control ($Smn^{+/-}$;$SMN2^{tg/0}$) and $n = 11$ for SMA animals ($Smn^{-/-}$; $SMN2^{tg/0}$); $SMN2^{tg}$ = two copies of *SMN2*. (**G**) *In situ* hybridization of miR-183 using LNA probes on 7 DIV spinal motor neurons with SMN-knockdown. Intensities of miR-183 signals were measured with ImageJ. The signals from neurites were normalized to the signal from cell body of individual neuron. N = 25 for control and $n = 20$ for *Smn*-knockdown neurons. Data are represented as mean ± SEM. Scale bar: 50 μm. Mature miRNA expression was normalized to snoRNA, *U6B*. Primary miRNA expressions were normalized to *Gapdh* expression. For neurites samples and sciatic nerve, 3 ng of total RNA was used to measure mRNA expression. Statistical significances were determined by student's *t*-test, $^{*}P < 0.05$, $^{**}P < 0.01$ and $^{***}P < 0.0001$.

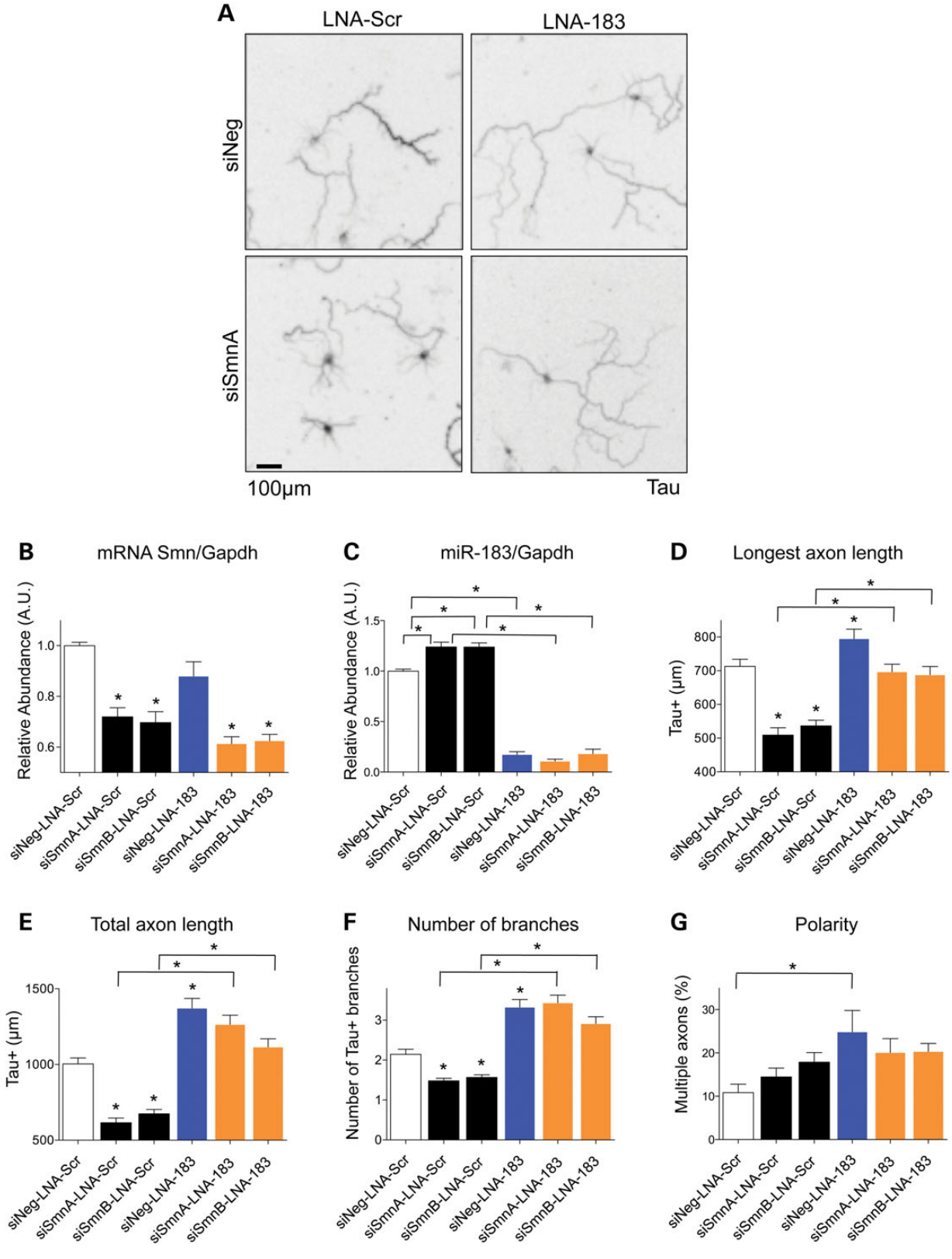

Figure 2. Knockdown of miR-183 expression with LNA inhibitor rescues neuronal morphology of SMN-deficient neurons. (**A**) Axonal morphology was visualized with Tau staining on 5 DIV. (**B**) Real-time PCR confirming efficiency of two different siRNAs against *Smn*. (**C**) LNA inhibitor against miR-183 after 4 days of transfection. $n = 8$, from four different experiments. (**D**) Length of the longest axon, (**E**) total length of axons, (**F**) number of axonal branches and (**G**) percentage of neurons with multiple axons. $n = 150–221$ from five different experiments. Data are represented as mean ± SEM. Student's *t*-test, $^{*}P < 0.05$. Scale bar: 100 µm.

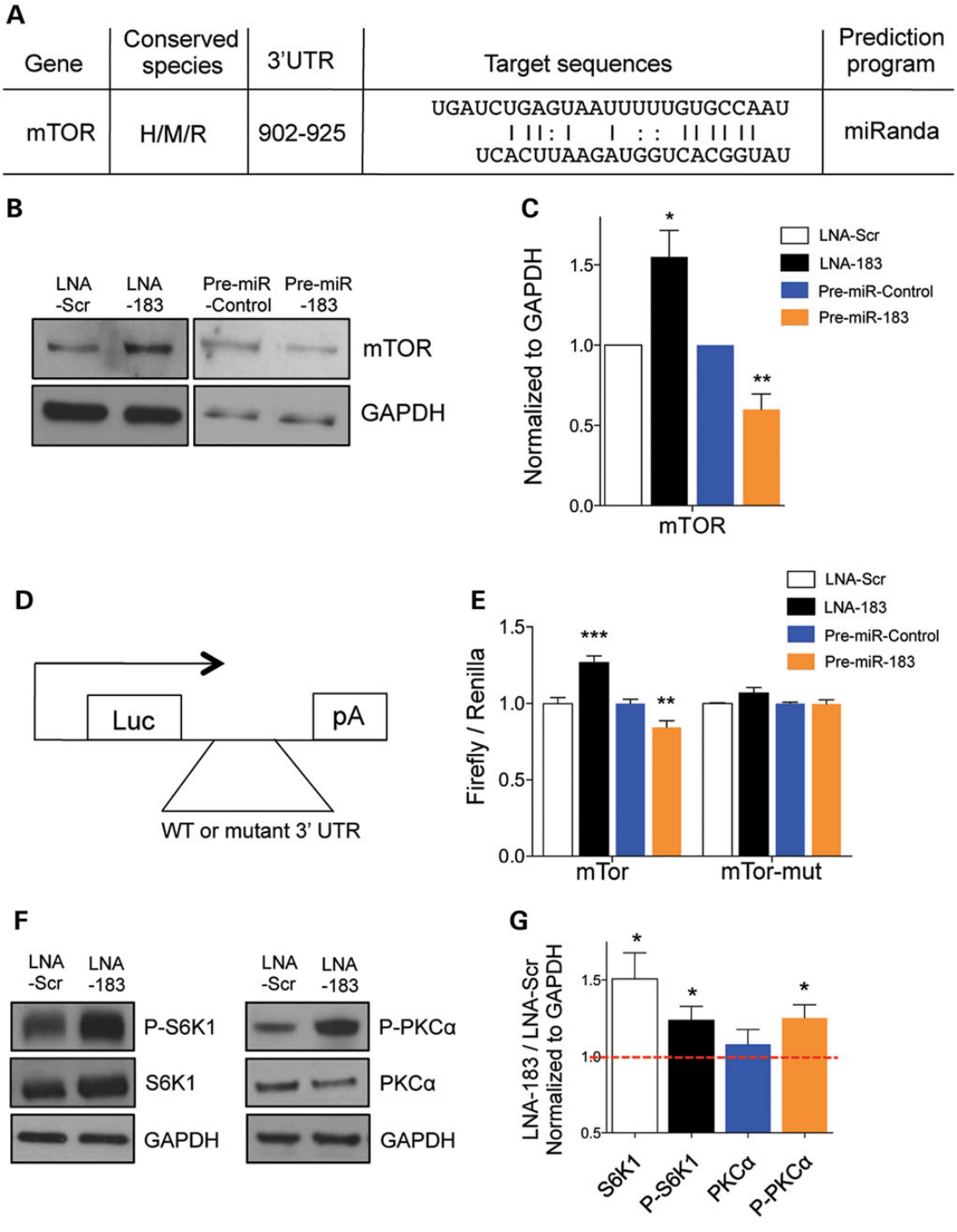

Figure 3. miR-183 directly regulates translation of *mTor*. (**A**) Putative binding sites for miR-183 in 3′ UTR of *mTor*. (**B**) Representative western blot showing that modification of miR-183 expression changes protein levels of mTOR in 48 h after transfection. (**C**) Quantification of protein normalized to GAPDH expression, $n = 6$ to nine experiments. Student's *t*-test, $^{*}P < 0.05$ and $^{**}P < 0.01$, compared with control samples. (**D**) Schematic figure of firefly luciferase reporter vector. (**E**) Firefly luciferase reporter assays of *mTor* 3′ UTRs with modifying miR-183 expression. Firefly luciferase activity is normalized to Renilla luciferase activity. Data represent relative expression of normalized firefly luciferase activity in miR-183 modified samples compared with control samples. $n = 8–16$, student's *t*-test, $^{**}P < 0.01$ and $^{***}P < 0.001$. (**F**) Western blots of proteins downstream of the mTOR pathway. (**G**) Bar graphs represent protein expression of 5 to 8 different biological samples. Red dotted line represents control level. Student's *t*-test, compared with control samples, $^{*}P < 0.05$. Data are represented as mean ± SEM.

the effect of miR-183 on the expression of luciferase reporter. From these data, we conclude that miR-183 can regulate translation of *mTor* by directly binding to its 3′ UTR (Fig. 3D and E).

mTOR kinase exists in two distinct functional complexes, mTOR Complex 1 (mTORC1) and mTOR Complex 2 (mTORC2), defined by two groups of binding partners (35).

Because mTOR is a core component of the two complexes, we asked how the activities of mTORC1 and mTORC2 were affected by loss of miR-183. It is well established that mTORC1 phosphorylates S6K1 at Thr389, and mTORC2 phosphorylates PKCα at Ser657 (36). Therefore, we measured phosphorylation of these two proteins as markers of mTORC1/2 activity. Interestingly, levels of S6K1 protein increased by ∼50% and the phosphorylated S6K1 (P-S6K1) increased ∼25% in miR-183 knockdown neurons. Moreover, phosphorylated PKCα (P-PKCα) increased ∼25%, whereas the total amount of PKCα protein was unchanged (Fig. 3F and G). These results indicate that both mTORC1 and mTORC2 are modulated by miR-183 expression in neurons.

Smn-knockdown neurons exhibit dysregulated mTOR activity and reduced protein synthesis

Having demonstrated an effect of miR-183 on the mTOR pathway, we examined whether SMN expression also modulates the expression and activity of the mTOR pathway in neurons. To investigate this question, we knocked down *Smn* and measured the expression of proteins in the mTOR pathway in cortical and spinal motor neurons. Protein levels of many genes in the mTOR pathway such as S6K1 and SGK were down-regulated in *Smn*-knockdown cells compared with controls in both cortical and spinal motor neurons (Fig. 4A–C). Based on the expression and phosphorylation of S6K1, S6 ribosomal subunit, SGK and PKC-α, we conclude that the activity of the mTOR pathway is reduced in cortical and spinal motor neurons with *Smn*-knockdown. As mTORC1 regulates protein synthesis, we asked whether SMN deficiency might cause impairment in protein synthesis. We used surface sensing of translation technology (SUnSET) to measure protein synthesis efficiency in cells (37). Interestingly, both *Smn*-knockdown neurons and neurons from the SMA mouse model showed reduced puromycin incorporation during 1 h of incubation, suggesting that SMN deficiency causes impairment in *de novo* protein synthesis efficiency (Fig. 4D, Supplementary Material, Fig. S5A). To test whether this is a neuron-specific phenomenon, we performed the same experiments with SMA patient-derived fibroblast cell

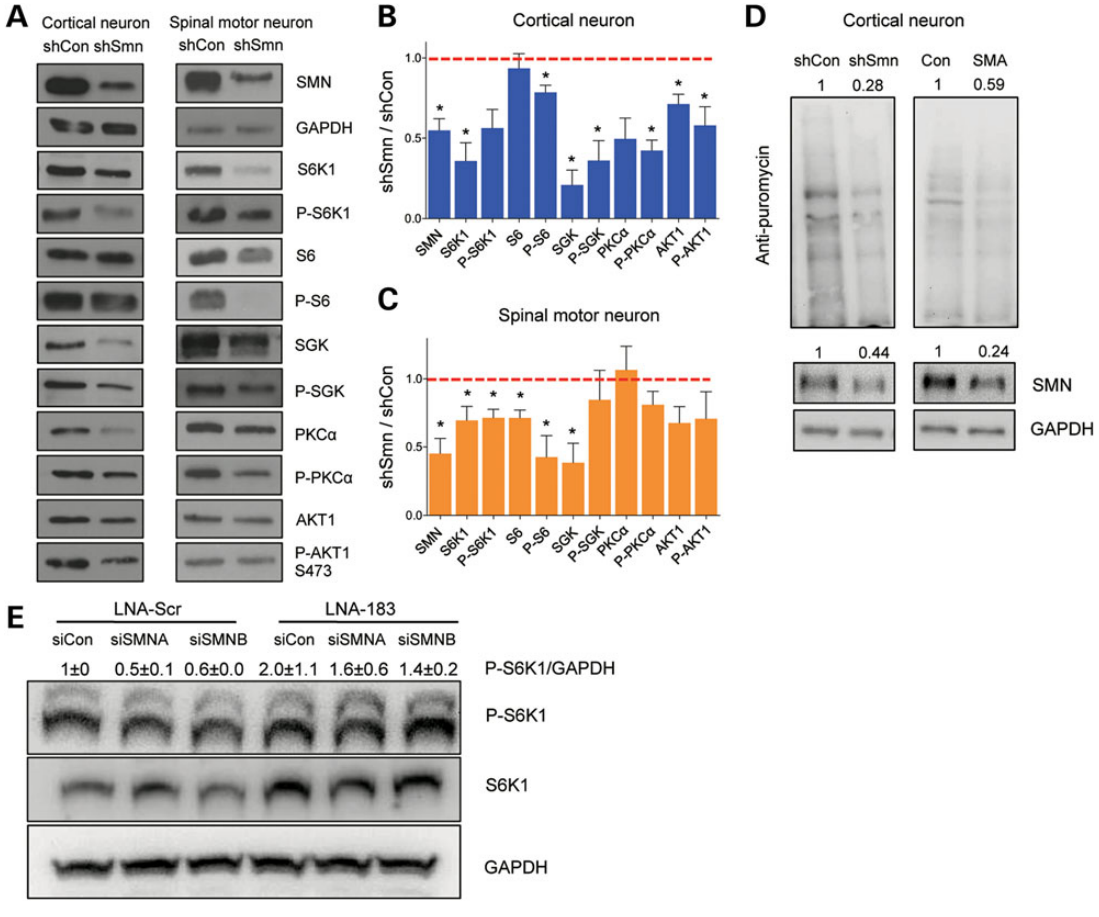

Figure 4. SMN deficiency impairs protein synthesis by dysregulation of mTOR activity in neurons. (**A**) Western blot of proteins in mTOR pathway. Neurons were infected by lentivirus expressing shRNA against *Smn* on 1 DIV. After 9 days (cortical neurons) and 6 days (spinal motor neurons) of infection, proteins were collected and analyzed by western blot. Bar graphs represent quantification of the expression of proteins involved in mTOR pathway in (**B**) cortical neurons and (**C**) spinal motor neurons. $n = 3–5$ for cortical neurons; $n = –9$ for spinal motor neurons, student's *t*-test, $^*P < 0.05$, compared with control lentivirus-infected neurons. Data are represented as mean ± SEM. (**D**) SUnSET experiments independently support that protein synthesis efficiency is reduced in SMN-deficient neurons. Experiments were performed either *Smn*-knockdown cortical neurons (shCon and shSMN) or cortical neurons from a SMA mouse model (Con and SMA). (**E**) miR-183 inhibition increased S6K1 phosphorylation in SMN-deficient neurons. 50 nM siRNA and 50 nM LNA inhibitors are transfected to cortical neurons. Western blots were repeated twice with two different biological samples. Data represent mean ± SEM.

lines. We measured P-S6K1 protein as a marker of mTORC1 activity. Surprisingly, even though these cell lines do not exhibit significant differences in cell growth and apoptosis compared with those from healthy controls, fibroblast cell lines derived from type 1 SMA patients showed reduced mTOR activity (Supplementary Material, Fig. S5B and C). These data indicate that reduced SMN protein expression leads to down-regulation of mTOR activity and impaired protein synthesis. To test whether reduced mTOR activity can be restored by inhibition of miR-183 in SMN-deficient neurons, we knocked down SMN and miR-183 simultaneously in cortical neurons and measured phosphorylation of S6K1. Indeed, inhibition of miR-183 in SMN-deficient neurons increased phosphorylation of S6K1 (Fig. 4E). These data support our hypothesis that down-regulated mTOR activity can be recovered by inhibition of miR-183.

mTOR is locally translated in the axon

As miR-183 levels are increased in neurites of *Smn*-knockdown neurons and miR-183 regulates mTOR activity via direct binding to the 3′ UTR of *mTor*, we asked whether *mTor* is locally translated in axons by performing fluorescence recovery after photobleaching (FRAP). We expressed plasmids with myristoylated photodestructible GFP fused to the 3′ UTR of *mTor* in hippocampal neurons. After 24 h, the GFP signals of the *mTor* reporter constructs could be detected in growth cones and axons. Two to three days after transfection, FRAP was performed using a laser confocal microscope with live cell imaging (Fig. 5A and Supplementary Material, Fig. S6A). The GFP signal was ∼50% recovered within 5 min after photobleaching, and anisomycin, a protein synthesis inhibitor, blocked this recovery (Fig. 5B). These data suggest that recovery of GFP signal in the axons is due to local protein synthesis (Fig. 5B).

To test whether SMN-deficient neurons also exhibit impaired local translation, we performed FRAP experiments with *mTor* reporter constructs in *Smn*-knockdown neurons. SMN-deficient neurons displayed impaired local translation for *mTor* (Fig. 5C). We then asked whether knocking down miR-183 could regulate local protein synthesis of mTOR in SMN-deficient neurons. Inhibition of miR-183 with LNA improved fluorescence recovery of *mTor* reporter constructs in SMN-deficient neurons (Fig. 5C), indicating an increase in the rate of local protein synthesis for mTOR following miR-183 inhibition. To independently test our finding that mRNAs of *mTor* is locally translated, we asked whether *mTor* mRNA is present in neurites. We measured endogenous mRNA levels for *mTor* in the neurite compartment isolated from Boyden chambers. We found that the levels of *mTor* mRNA is similar to those of the well-established axonal mRNA *β-actin* (Supplementary Material, Fig. S6B). From these results, we conclude that expression of mTOR is regulated at the translational level in distal neurites.

Inhibition of miR-183 in spinal motor neurons improves SMA mouse model

Finally, we asked whether suppression of miR-183 could alter the phenotype of an SMA mouse model. To test this, we produced an adeno-associated virus serotype-9 (AAV9) vector carrying a sponge sequence that would bind to and inhibit miR-183 expression following CNS injections of SMA mice. This vector

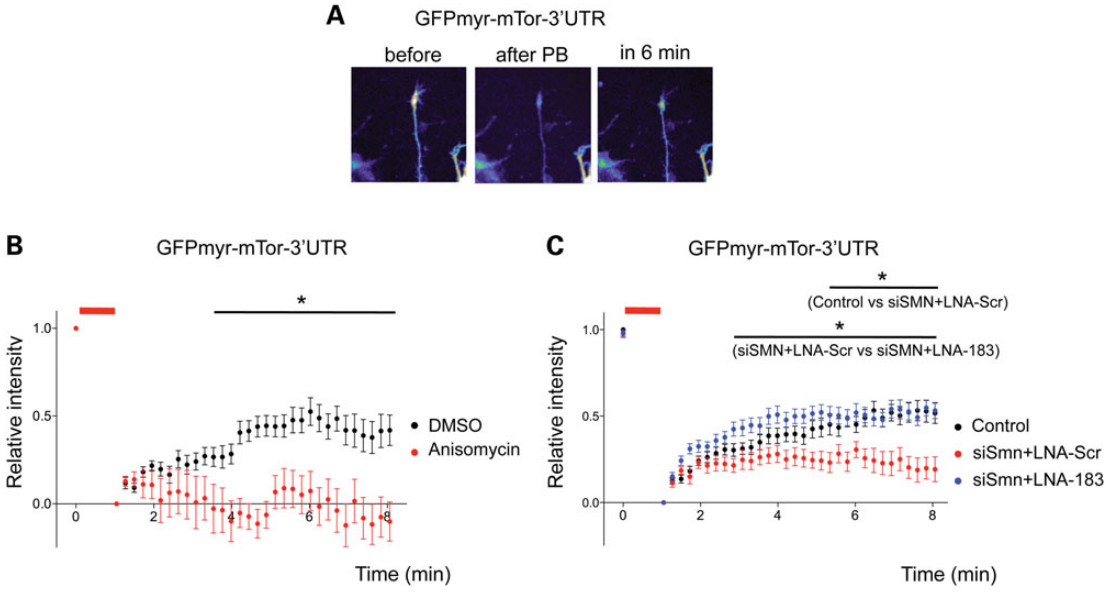

Figure 5. *mTor* is locally translated in the axon and growth cones. (**A**) Representative images demonstrate FRAP in distal axons of hippocampal neurons transfected with dGFPmyr-*mTor* 3′ UTR over a period of 6 min. (**B**) Quantification of GFP intensity of dGFPmyr-*mTor*-3′ UTR in the distal axons and growth cones before and after photobleaching (PB). Anisomycin (50 μM, red) blocked recovery of GFP signal after PB compared with vehicle-treated neurons (DMSO, black). For each time point, the data represent a relative ratio of prebleach intensity (mean ± SEM). DMSO: $n = 33$ regions from 11 neurons, anisomycin: $n = 17$ regions from 5 neurons. Statistical significance was determined by two-way ANOVA followed by Bonferroni's *post hoc* test. DMSO versus anisomycin: $^*P < 0.05$ from 3.99 to 8.06 min (**C**) *Smn*-knockdown neurons showed significantly reduced recovery of GFP signal, and inhibition of miR-183 in *Smn*-deficient neurons restored it. Control (black): $n = 52$ from 19 neurons, *Smn*-knockdown (red): $n = 52$ from 17 neurons and *Smn* and miR-183 double knockdown (blue): $n = 44$ from 12 neurons. Control versus siSMN + LNA-Scr; $^*P < 0.05$ from 5.35 to 8.06 min, siSMN + LNA-Scr versus siSMN + LNA-183; $^*P < 0.05$ from 2.86 to 8.06 min. Red bars represent times of photobleaching.

has a beta-glucuronidase (GUSB) promoter that expresses primarily in neurons (38), thus allowing us to restrict the inhibition of miR-183 expression in spinal motor neurons and interneurons. AAV9-sponge-183 reduced miR-183 expression to <40% of wild-type levels (from 1.3 to 0.5, compared with wild-type control) (Fig. 6A). As miR-182 has very similar sequence with miR-183, we also measured miR-182 expression as a control. miR-183 sponge sequence did not change miR-182 expression significantly. Remarkably, reduction of miR-183 in the spinal cord extended the survival of SMA mice from an average of 16.5–19.5 days (Fig. 6B). Additionally, inhibition of miR-183 partially improved body weight and motor function, as measured by grip test (Fig. 6C and D). However, there was no significant increase in righting reflex (Fig. 6E). Immunofluorescent staining confirmed that AAV9-sponge-183 virus infected motor neurons in spinal cord (Fig. 6F). Despite the physiological improvement in miR-183 inhibited SMA animals, we did not detect significant differences in NMJ morphology or survival of motor neurons (Supplementary Material, Fig. S7A–D).

DISCUSSION

Local mRNA translation plays an important role in neuronal development and synaptic plasticity, and its dysregulation can contribute to neurological disorders such as Fragile X Syndrome

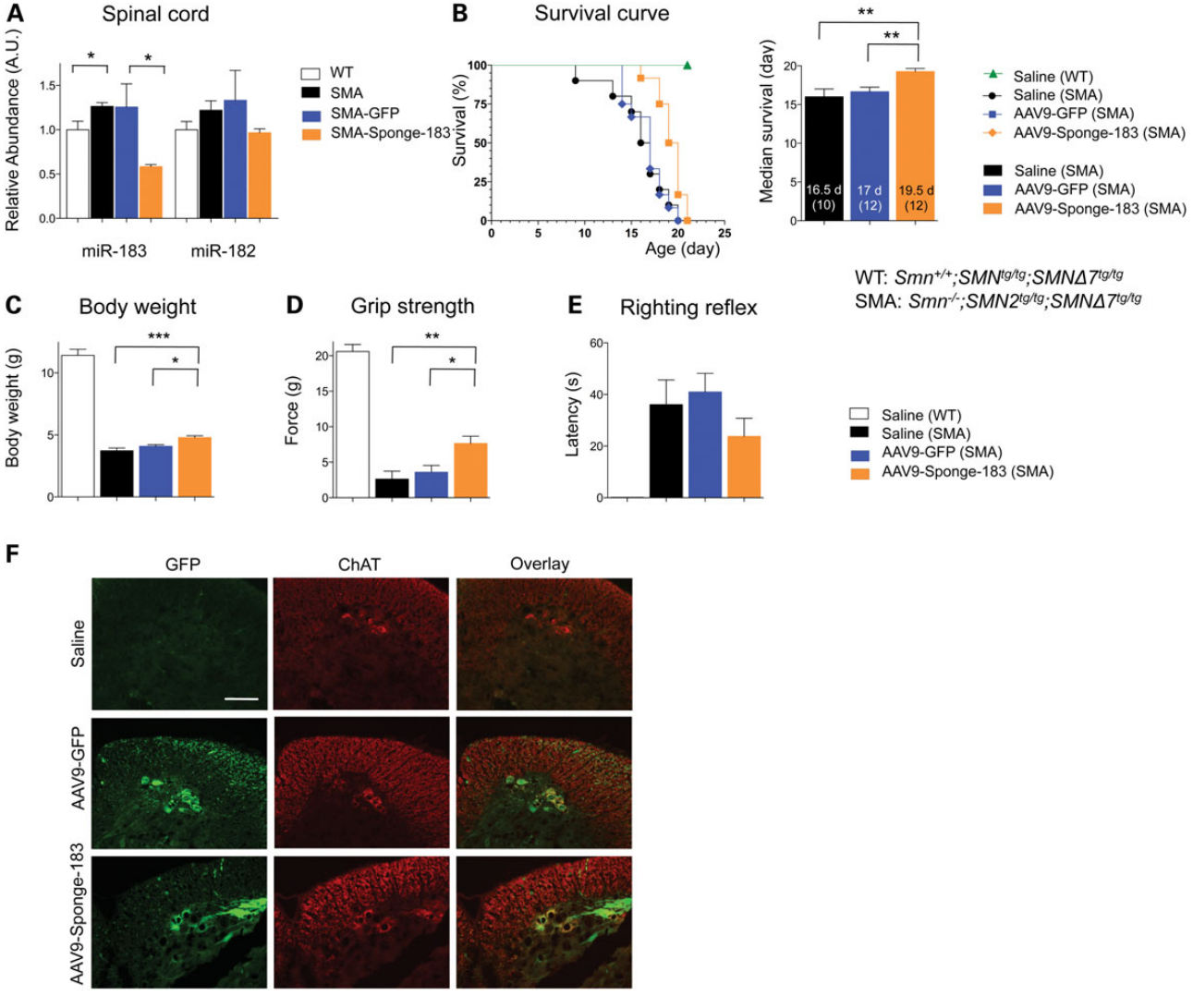

Figure 6. AAV-sponge-mediated inhibition of miR-183 in spinal motor neurons improved survival, body weight and motor function in a mouse model of SMA. AAV9-Sponge-183, AAV9-GFP or saline was injected into the CNS of SMA mice on the day of birth. One cohort of mice was sacrificed on postnatal day 14 for age-matched expression analysis (**A**, **F**), and a second cohort of mice was analyzed for behavior and survival (**B**–**E**). (**A**) AAV9-Sponge-183 restored miR-183 expression in the spinal cord of SMA mice. Expression of miR-182, a miRNA from the same cluster and with a similar sequence did not show significant reduction. (**B**) Survival and behavior of animals. $n = 10$ for saline-injected animals with median survival 16.5 days, $n = 12$ for AAV9-GFP control with median survival of 17 days, and $n = 12$ for AAV9-Sponge-183-injected animals with median survival 19.5 days. Statistical significance was determined by log-rank (Mantel–Cox) test and $^{**}P < 0.01$. (**C**) Body weight, (**D**) grip strength and (**E**) righting reflex were measured at postnatal day 14. Statistical significance was determined by one-way ANOVA followed by Bonferroni's Multiple Comparison test, $^{***}P < 0.001$, $^{*}P < 0.05$. (**F**) Fluorescent microscopy of the lumbar spinal cord of SMA mouse shows that AAV9 (GFP) was successfully delivered to motor neurons (ChAT).

and SMA (25). Dysfunction of translational machinery has been shown to contribute to neurological diseases. For example, hyperactivation of mTOR plays an important role in the neuropathology of tuberous sclerosis and PTEN hamartoma syndromes (25,39). Moreover, dysregulation of miRNA-mediated translational repression has been implicated in many neurodegenerative diseases, including Alzheimer's and Huntington's diseases (40,41). However, the interplay between miRNA expression and the mTOR pathway has not been studied in motor neuron diseases, especially with respect to the axonal local translation. Here, we report a previously unappreciated relationship between SMN, miRNA expression and mTOR signaling.

In vivo experiments show that modulating mTOR levels via miR-183 knockdown is a potential target for adjunctive treatment in a severe mouse model of SMA. Although reducing miR-183 resulted in a significant increase in grip strength and median survival, we were not able to detect differences in gross NMJ morphology compared with control SMA mice. Future studies are needed to investigate the possibility that subtle changes in the NMJ structure and/or function might have contributed to the observed improvement in motor function and longevity.

The mechanisms by which SMN deficiency leads to dysregulation of miRNA expression/localization and mTOR activity are unclear. The predominant mechanism for miR-183 dysregulation appears to be post-transcriptional because the transcription of miR-183∼96∼182 cluster is unchanged, and miR-182 from the same gene cluster is not affected by SMN loss. There are several possible explanations for this observation. First, as SMN plays a major role in splicing, incorrect splicing of genes important for miRNA biogenesis could lead to aberrant miRNA expression/distribution. Second, the SMN complex is involved in the formation of ribonucleoproteins (RNPs) (42,43). Recently, our lab and others showed that SMN complex binds to the RNA-binding protein HuD and delivers mRNAs to the axonal compartment to be translated locally (14,19). The SMN complex may play a role in the formation or trafficking of miRNA–RISC complexes and/or translational machinery. Third, loss of SMN may potentiate cellular stress mechanisms. The SMN complex is necessary for stress granule formation and function in neurons (44). As stress granules may regulate miRNA function by sequestering Argonaute, RNA-binding proteins and RNA editing enzymes (45), their dysfunction could also affect miRNA expression and distribution. Regardless of the mechanism, there appears to be specificity for certain miRNAs, suggesting that the distribution of different miRNAs may depend on distinct processing and transport mechanisms. Identification of RNP complexes involved in transport and processing of different miRNAs could help elucidate these mechanisms.

Another important consideration is that the role of mTOR-related protein synthesis in growing neurons, including mRNA translation of mTOR pathway components, is regulated locally in developing axons. There have been numerous studies reporting that the mTOR pathway plays a role in axonal outgrowth (25,28). In this study, we demonstrated that *mTor* itself is locally translated in the developing axon. Local synthesis of the mTOR protein that is the master regulator of protein synthesis has important implications. One would predict that down-regulated mTOR signaling in SMN-deficient cells would markedly repress protein synthesis machinery, leading to neuronal dysfunction and aberrant neuronal connectivity.

Several recent studies demonstrated roles for miRNAs in axonal growth, which are consistent with our findings. For example, the miR-17∼92 cluster increased axonal outgrowth by repressing PTEN expression in embryonic cortical neurons, and miR-16 regulates protein synthesis at the sympathetic neuronal axons by inhibiting translation of eIF2B2 and eIF4G2 (46,47). At the neuromuscular junction, miR-124 and miR-142 modulate acetylcholine release via Rab3a, which is involved in synaptic vesicle delivery in response to elevated NO signals from postsynaptic skeletal muscle (48). Motor neurons differentiated from murine embryonic stem cells harboring a mutation causing SMA showed dysregulation in miR-9 expression (24). Interestingly, miR-9 regulates axonal growth via regulation of MAP1b expression in neurons (49). Dysregulated miR-9 expression in SMA neurons might also contribute to pathological axonal morphology in SMA. These findings, together with our data, strongly suggest that axon growth and axonal local translation are regulated by miRNAs and are dysregulated in SMA.

We demonstrate that inhibition of miR-183 rescues much of the neuronal phenotype associated with *Smn*-knockdown, particularly axon outgrowth. miR-183 increases mTOR pathway activity, which contributes to this effect, but miR-183 may have additional targets that also augment this result. Our findings are consistent with previous reports demonstrating that PTEN deletion in SMA neurons improved neuronal growth (50) and that IGF-1 enhanced survival of SMA mice (51,52). Our study provides a potential link between the SMN/miR-183/mTOR interaction and the SMA neuronal phenotype. Most of the therapeutic strategies in SMA have focused on increasing SMN levels (38,53). Although our AAV9-sponge-183 modestly decreased miR-183 expression to 50% of wild type, we nonetheless observed an improvement in a mouse model of SMA. Inhibition of miR-183 alone unlikely provides a cure for SMA, but it may work in concert with other therapeutic modalities that are aimed to increase SMN protein levels in cells. Whether similar mechanisms are in play in human SMA disease requires future investigations. If they are, then more efficient, cell-type-specific modulation of the mTOR pathway via small molecules or RNAi could potentially provide a new mechanism-based adjunctive therapy for this devastating disease.

MATERIALS AND METHODS

Primary neuron cultures

All experimental procedures were performed in compliance with animal protocols approved by the IACUC at Boston Children's Hospital and University of Cologne. Hippocampi and cortices were dissected from E18 Sprague–Dawley rat embryos (Charles River). Neurons were dissociated with papain, triturated and plated on poly-D-lysine/Laminin-coated plates. Cells were plated at 1 M ∼ 250 K cells/6-well plates for biochemistry and 30 000 cells/24 well plates for immunostaining experiments. Neurons were cultured in Neurobasal medium with B27 supplement, 2 mM L-glutamine, 1 × pen-strep (Invitrogen) at 37°C in a humidified incubator with 5% CO_2. For the motor neuron culture, we used embryonic spinal motor neuron from E15 Sprague–Dawley rat embryos (Charles River). Primary motor

neurons were cultured with same media with 50 ng/μl BDNF, 50 ng/μl GDNF and 25 ng/μl CNTF (PeproTech) as described before (14).

Boyden chamber and collection of samples from neurite compartment

Cortical neurons were cultured on modified Boyden chambers as described previously (28). In brief, neurons were seeded on the Boyden membrane with 3-μm pores with Neurobasal media with B27 supplement, 2 mM L-glutamine and 1 × pen-strep (Invitrogen). We added this culture media with BDNF (50 ng/μl), CNTF (50 ng/μl) and GDNF (25 ng/μl) to the lower compartment of the culture dishes. One day after seeding, cells were infected with lentivirus containing either the shRNA against *Smn* or the scramble control (14). Samples were collected 9 days after infection from both the lower membrane surface, which contained mainly the neurite compartment and growth cones, and the upper membrane surface, which contained cell bodies.

RNA extraction and measuring expression of mRNAs

Total RNA was extracted using *miRVana* total RNA isolation kit (Ambion) according to manufacturer's instruction. RNA amount was measured using Nanodrop (Thermo Scientific). To measure the expression of mRNAs, we used a previously described protocol (54). In brief, 120 ng of total RNA was reversed-transcribed using cDNA Archiving Kit with random primers (Life Tech). Power SyBr Green PCR Master Mix (Life Tech) was used to amplify and detect signals with 10 ng of cDNA and 1 mM of each gene-specific primer. Sequences of individual primers for mRNA detection are in Supplementary Material, Table S7. Amplified signals were collected by 7300HT fast real-time System (ABI) and normalized with *Gapdh* intensity.

Multiplexed real-time PCR for miRNA analysis and single miRNA analysis

miRNA expression was also measured using multiplexed real-time PCR as described before (7). In brief, 187-plexed real-time PCR was used to measure the expression of individual miRNAs. Twenty nanograms of total RNA was reverse-transcribed using cDNA Archiving Kit (Life Tech) and 2.5 nM miRNA-specific reverse primers. cDNA was pre-amplified using a common reverse primer (UR) and miRNA-specific forward primers using Universal Master Mix with no UNG (Life Tech). PCR product was diluted 4 times, and 0.1 μl was used for real-time PCR. Real-time PCR was performed in 7500HT fast real-time System (ABI). To measure individual miRNA expression, we used Taqman microRNA assays (Lite Tech). Data were collected and analyzed as previously described (54). Threshold cycles (Ct) were normalized by a single proportionality constant as we did not observe any Ct-dependent bias.

Western blotting

Protein expression was quantified by western blotting. Antibodies used for this study were purchased from phospho-PKCa (Ser657, Millipore), phospho-S6K1 (Ser389, Millipore), phospho-SGK (Ser255/Thr256, Millipore), Akt1 (Santa Cruz), SMN (Santa Cruz), mTOR (Cell Signaling), phospho-Akt1 (Ser473, Cell Signaling), PKCα (Cell Signaling), S6 (Cell Signaling), phospho-S6 (Ser240/244, Cell Signaling), S6K1 (Cell Signaling), SGK (Abcam), Tau (Millopore), RIP1 (Cell Signaling), Caspase 3 (Cell Signaling), Lamin B1 (Abcam) and GAPDH (Ambion).

3′ UTR reporter system, site directed mutagenesis and luciferase assay

We amplified 3′ UTR of mTOR from the rat genomic DNA and cloned into pmiR-report vector (Ambion). Three hundred nanograms of reporter vectors were transiently transfected to HEK293T cells together with 50 ng of control vector expressing Renilla luciferase and 50 nM of pre-miRNA (AB) or LNA inhibitors (Exiqon) using Lipofectamine2000 (Life Tech). In 24 h after transfection, cells were harvested and luciferase activity was measured with Dual luciferase system (Promega). To construct reported vector containing mutations in miRNA seed region, we used QuickChange II XL Site Directed Mutagenesis Kit (Agilent). In brief, we designed primers containing inverted sequences of 6 base pairs in seed region (IDT) and followed manufacturer's instruction for detailed procedures. Primer sequences used to make point mutation are for mTOR 3′ UTR, forward primer: 5′ GTATCTGAGTAATTTTTACCGTGATAAATGACATCAG 3′; reverse primer: 5′ CTGATGTCATTTATCACGGTAAAAATTACTCAGATAC 3′.

In situ hybridization of miR-183 using LNA probe and image analysis

We performed *in situ* hybridization of miR-183 with LNA probes as previously described (7). We used 57°C as a hybridization temperature, which is 20°C below Tm of our LNA probes. Images were taken with Zeiss Axio ImagerM2, and miR-183 signals from neurites were measured with ImageJ. We measured signals from neurites at least 25 μm away from cell body.

Lentiviral production and infection

Lentiviral particles were produced in HEK293T cells as described before (55). In brief, lentiviral plasmids were transiently transfected with packaging vectors using Lipofectamine2000 and OptiMEM (Life Tech). Lentiviral particles were collected 48 h after transfection.

Immunostaining and axon length measurement

Neurons were fixed and stained with Tau antibody (Millipore) to measure axonal morphology. Tau-positive neurites were measured using ImageJ.

miRNA inhibition in cultured neuron using transient transfection

We designed inhibitors of miRNA using Locked Nucleic Acid technology (LNA, Exiqon). LNA sequence to inhibit expression of miR-183 was +A +G +T +G +AATTCTACCAGTG +C +C +A +T +A. For the negative control, we used +C +A +T

+T +AATGTCGGACAAC +T +C +A +A +T ('+' = locked base). We transiently transfected LNA oligonucleotides using Lipofectamine2000 reagent and OptiMEM (Invitrogen) on 1 DIV. For transfection protocol, we followed the manufacturer's instructions.

Protein synthesis efficiency (SUnSET experiment)

Primary cultured neurons were incubated with 50 μM puromycin, 1 h in their culture medium and protein was extracted. Incorporated puromycin was quantified with anti-puromycin antibody (KeraFest) by western blot. Twenty micrograms of proteins were used for western analysis (37). Western blot images were quantified with ImageJ.

Sponge-183 AAV production and injection

The sponge-183 sequence was cloned into a shuttle plasmid that contained the eGFP cDNA, the 0.4-kb human GUSB promoter and the self-complementary AAV2 inverted terminal repeats. The sponge-183 sequence consisted of seven bulged binding sites for miR-183 and four nucleotide spacer sequences (CCGG) between them [5′ CAGTGAATTCTTATGTGCCATACCGG CAGTGAATTCTTATGTGCCATACCGGCAGTGAATTCTT ATGTGCCATACCGGCAGTGAATTCTTATGTGCCATACCGG CAGTGAATTCTTATGTGCCATACCGGCAGTGAATTCT TATGTGCCATACCGGCAGTGAATTCTTATGTGCCATA 3′ (56)]. The recombinant plasmid was packaged into AAV serotype-9 capsid by triple-plasmid co-transfection of HEK293 cells to generate AAV9-sponge-183 (scAAV2/9-GUSB-GFP-sponge-183). The negative control vector, AAV9-GFP (scAAV2/9-GUSB-GFP), was identical except that it did not contain the sponge-183 sequence. All animal procedures were performed under a protocol approved by the Institutional Animal Care and Use Committee. On the day of birth (P0), pups received 2 μl into each the right and left cerebral lateral ventricles and into the lumbar spinal cord for a total volume of 6 μl and a total dose of 2.5e10 genome copies per pup. All the injections were performed with a finely drawn glass micropipette needle as described earlier (57). A subset of the litters was treated with saline to control for the injection procedure. Following the injections, the pups were toe-clipped and genotyped to identify SMA ($Smn^{-/-}$, $hSMN2^{+/+}$, $SMND7^{+/+}$), heterozygote ($Smn^{+/-}$, $hSMN2^{+/+}$, $SMND7^{+/+}$) and wild-type ($Smn^{+/+}$, $hSMN2^{+/+}$, $SMND7^{+/+}$) mice. Behavioral tests and tissue analyses were performed as reported (57).

Fluorescence recovery after photobleaching

3′ UTR of *mTor* was cloned into myristoylated GFP vectors to measure local translation in neurons (gift from Dr Jeffery Twiss), as described previously (28). In brief, 3′ UTR:myrGFP vectors were transfected into neurons using Amaxa nucleofection (Lonza). We followed the manufacturer's instruction for experimental procedures. Two days after transfection, images were collected using Zeiss LSM5 confocal microscopy with a 37°C platform and analyzed with Zen (Zeiss). For anisomycin treatment, neurons were incubated with vehicle (DMSO) or anisomycin (50 ng/ml) for 30 min before imaging. Statistical significance was determined with two-way ANOVA followed by Bonferroni's *post hoc* test.

SUPPLEMENTARY MATERIAL

Supplementary Material is available at *HMG* online.

ACKNOWLEDGEMENTS

We thank members of the Sahin lab, Drs Larry Benowitz and Elizabeth Engle for critical reading of the manuscript. We thank Jason Steinberg, Abbey Sadowski, Sam Goldman, Emily Greene-Colozzi, Jarrett Leech, Jie Bu and Amy Richards for technical assistance. Human tissue was obtained from the Pediatric Neuromuscular Clinical Research Network (PNCRN). The role of the PNCR tissue repository is to distribute tissue and therefore cannot endorse the studies performed or the interpretation of the results.

Conflicts of Interest statement: Marco Passini and Pablo Sardi are paid employees of Genzyme, a Sanofi Company.

FUNDING

This work is supported in part by grants of the Slaney Family Fund, Whitehall Foundation and Boston Children's Hospital (BCH) Translational Research Program to M.S., and the BCH Intellectual and Developmental Disabilities Research Center (P30 HD18655). M.K. was supported by a grant from the Harvard NeuroDiscovery Center and fellowship from the Hearst Foundation. E.D.N. received support from the Developmental Neurology Training Grant (T32 NS007473). P.N.'s research was supported in part by the National Science Foundation under Grant No. PHY05-51164. B.W. was supported by grants of the Deutsche Forschungsgemeinschaft Wi945-14/1 and the EU FP7/2007-2013 program under grant agreement no 2012-305121 (Project acronym NeurOmics), the CMMC project no C11 and M.R. by SMA-Europe. U.M. was supported by grants from SMA-Europe, fSMA, MDA and R01 NS057482.

REFERENCES

1. Sengupta, S., Nie, J., Wagner, R.J., Yang, C., Stewart, R. and Thomson, J.A. (2009) MicroRNA 92b controls the G1/S checkpoint gene p57 in human embryonic stem cells. *Stem Cells*, **27**, 1524–1528.
2. Conaco, C., Otto, S., Han, J.J. and Mandel, G. (2006) Reciprocal actions of REST and a microRNA promote neuronal identity. *Proc. Natl. Acad. Sci. USA*, **103**, 2422–2427.
3. Gao, J., Wang, W.Y., Mao, Y.W., Graff, J., Guan, J.S., Pan, L., Mak, G., Kim, D., Su, S.C. and Tsai, L.H. (2010) A novel pathway regulates memory and plasticity via SIRT1 and miR-134. *Nature*, **466**, 1105–1109.
4. Konopka, W., Kiryk, A., Novak, M., Herwerth, M., Parkitna, J.R., Wawrzyniak, M., Kowarsch, A., Michaluk, P., Dzwonek, J., Arnsperger, T. *et al.* (2010) MicroRNA loss enhances learning and memory in mice. *J. Neurosci.*, **30**, 14835–14842.
5. Landthaler, M., Gaidatzis, D., Rothballer, A., Chen, P.Y., Soll, S.J., Dinic, L., Ojo, T., Hafner, M., Zavolan, M. and Tuschl, T. (2008) Molecular characterization of human Argonaute-containing ribonucleoprotein complexes and their bound target mRNAs. *RNA*, **14**, 2580–2596.
6. Murashov, A.K., Chintalgattu, V., Islamov, R.R., Lever, T.E., Pak, E.S., Sierpinski, P.L., Katwa, L.C. and Van Scott, M.R. (2007) RNAi pathway is functional in peripheral nerve axons. *FASEB J.*, **21**, 656–670.

7. Kye, M.J., Liu, T., Levy, S.F., Xu, N.L., Groves, B.B., Bonneau, R., Lao, K. and Kosik, K.S. (2007) Somatodendritic microRNAs identified by laser capture and multiplex RT-PCR. *RNA*, **13**, 1224–1234.
8. Natera-Naranjo, O., Aschrafi, A., Gioio, A.E. and Kaplan, B.B. (2010) Identification and quantitative analyses of microRNAs located in the distal axons of sympathetic neurons. *RNA*, **16**, 1516–1529.
9. Banerjee, S., Neveu, P. and Kosik, K.S. (2009) A coordinated local translational control point at the synapse involving relief from silencing and MOV10 degradation. *Neuron*, **64**, 871–884.
10. Yoon, B.C., Zivraj, K.H. and Holt, C.E. (2009) Local translation and mRNA trafficking in axon pathfinding. *Results Probl. Cell. Differ.*, **48**, 269–288.
11. Wirth, B., Garbes, L. and Riessland, M. (2013) How genetic modifiers influence the phenotype of spinal muscular atrophy and suggest future therapeutic approaches. *Curr. Opin. Genet. Dev.*, **23**, 330–338.
12. Burghes, A.H. and Beattie, C.E. (2009) Spinal muscular atrophy: why do low levels of survival motor neuron protein make motor neurons sick? *Nat. Rev. Neurosci.*, **10**, 597–609.
13. Zhang, H., Xing, L., Rossoll, W., Wichterle, H., Singer, R.H. and Bassell, G.J. (2006) Multiprotein complexes of the survival of motor neuron protein SMN with Gemins traffic to neuronal processes and growth cones of motor neurons. *J. Neurosci.*, **26**, 8622–8632.
14. Akten, B., Kye, M.J., Hao le, T., Wertz, M.H., Singh, S., Nie, D., Huang, J., Merianda, T.T., Twiss, J.L., Beattie, C.E. *et al.* (2011) Interaction of survival of motor neuron (SMN) and HuD proteins with mRNA cpg15 rescues motor neuron axonal deficits. *Proc. Natl. Acad. Sci. USA*, **108**, 10337–10342.
15. Pellizzoni, L., Kataoka, N., Charroux, B. and Dreyfuss, G. (1998) A novel function for SMN, the spinal muscular atrophy disease gene product, in pre-mRNA splicing. *Cell*, **95**, 615–624.
16. Charroux, B., Pellizzoni, L., Perkinson, R.A., Shevchenko, A., Mann, M. and Dreyfuss, G. (1999) Gemin3: a novel DEAD box protein that interacts with SMN, the spinal muscular atrophy gene product, and is a component of gems. *J. Cell Biol.*, **147**, 1181–1194.
17. Charroux, B., Pellizzoni, L., Perkinson, R.A., Yong, J., Shevchenko, A., Mann, M. and Dreyfuss, G. (2000) Gemin4. A novel component of the SMN complex that is found in both gems and nucleoli. *J. Cell Biol.*, **148**, 1177–1186.
18. Mourelatos, Z., Dostie, J., Paushkin, S., Sharma, A., Charroux, B., Abel, L., Rappsilber, J., Mann, M. and Dreyfuss, G. (2002) miRNPs: a novel class of ribonucleoproteins containing numerous microRNAs. *Genes Dev.*, **16**, 720–728.
19. Fallini, C., Zhang, H., Su, Y., Silani, V., Singer, R.H., Rossoll, W. and Bassell, G.J. (2011) The survival of motor neuron (SMN) protein interacts with the mRNA-binding protein HuD and regulates localization of poly(A) mRNA in primary motor neuron axons. *J. Neurosci.*, **31**, 3914–3925.
20. Hubers, L., Valderrama-Carvajal, H., Laframboise, J., Timbers, J., Sanchez, G. and Cote, J. (2011) HuD interacts with survival motor neuron protein and can rescue spinal muscular atrophy-like neuronal defects. *Hum. Mol. Genet.*, **20**, 553–579.
21. Piazzon, N., Rage, F., Schlotter, F., Moine, H., Branlant, C. and Massenet, S. (2008) In vitro and in cellulo evidences for association of the survival of motor neuron complex with the fragile X mental retardation protein. *J. Biol. Chem.*, **283**, 5598–5610.
22. Tadesse, H., Deschenes-Furry, J., Boisvenue, S. and Cote, J. (2008) KH-type splicing regulatory protein interacts with survival motor neuron protein and is misregulated in spinal muscular atrophy. *Hum. Mol. Genet.*, **17**, 506–524.
23. Trabucchi, M., Briata, P., Garcia-Mayoral, M., Haase, A.D., Filipowicz, W., Ramos, A., Gherzi, R. and Rosenfeld, M.G. (2009) The RNA-binding protein KSRP promotes the biogenesis of a subset of microRNAs. *Nature*, **459**, 1010–1014.
24. Haramati, S., Chapnik, E., Sztainberg, Y., Eilam, R., Zwang, R., Gershoni, N., McGlinn, E., Heiser, P.W., Wills, A.M., Wirguin, I. *et al.* (2010) miRNA malfunction causes spinal motor neuron disease. *Proc. Natl. Acad. Sci. USA*, **107**, 13111–13116.
25. Liu-Yesucevitz, L., Bassell, G.J., Gitler, A.D., Hart, A.C., Klann, E., Richter, J.D., Warren, S.T. and Wolozin, B. (2011) Local RNA translation at the synapse and in disease. *J. Neurosci.*, **31**, 16086–16093.
26. Fallini, C., Bassell, G.J. and Rossoll, W. (2012) Spinal muscular atrophy: the role of SMN in axonal mRNA regulation. *Brain Res.*, **1462**, 81–92.
27. Rossoll, W., Jablonka, S., Andreassi, C., Kroning, A.K., Karle, K., Monani, U.R. and Sendtner, M. (2003) Smn, the spinal muscular atrophy-determining gene product, modulates axon growth and localization of beta-actin mRNA in growth cones of motoneurons. *J. Cell Biol.*, **163**, 801–812.
28. Nie, D., Di Nardo, A., Han, J.M., Baharanyi, H., Kramvis, I., Huynh, T., Dabora, S., Codeluppi, S., Pandolfi, P.P., Pasquale, E.B. *et al.* (2010) Tsc2-Rheb signaling regulates EphA-mediated axon guidance. *Nat. Neurosci.*, **13**, 163–172.
29. Willis, D., Li, K.W., Zheng, J.Q., Chang, J.H., Smit, A., Kelly, T., Merianda, T.T., Sylvester, J., van Minnen, J. and Twiss, J.L. (2005) Differential transport and local translation of cytoskeletal, injury-response, and neurodegeneration protein mRNAs in axons. *J. Neurosci.*, **25**, 778–791.
30. Kerr, D.A., Nery, J.P., Traystman, R.J., Chau, B.N. and Hardwick, J.M. (2000) Survival motor neuron protein modulates neuron-specific apoptosis. *Proc. Natl. Acad. Sci. USA*, **97**, 13312–13317.
31. Chen, W.W., Yu, H., Fan, H.B., Zhang, C.C., Zhang, M., Zhang, C., Cheng, Y., Kong, J., Liu, C.F., Geng, D. *et al.* (2012) RIP1 mediates the protection of geldanamycin on neuronal injury induced by oxygen-glucose deprivation combined with zVAD in primary cortical neurons. *J. Neurochem.*, **120**, 70–77.
32. Riessland, M., Ackermann, B., Forster, A., Jakubik, M., Hauke, J., Garbes, L., Fritzsche, I., Mende, Y., Blumcke, I., Hahnen, E. *et al.* (2010) SAHA ameliorates the SMA phenotype in two mouse models for spinal muscular atrophy. *Hum. Mol. Genet.*, **19**, 1492–1506.
33. Weeraratne, S.D., Amani, V., Teider, N., Pierre-Francois, J., Winter, D., Kye, M.J., Sengupta, S., Archer, T., Remke, M., Bai, A.H. *et al.* (2012) Pleiotropic effects of miR-183∼96∼182 converge to regulate cell survival, proliferation and migration in medulloblastoma. *Acta Neuropathol.*, **123**, 539–552.
34. Choi, Y.J., Di Nardo, A., Kramvis, I., Meikle, L., Kwiatkowski, D.J., Sahin, M. and He, X. (2008) Tuberous sclerosis complex proteins control axon formation. *Genes Dev.*, **22**, 2485–2495.
35. Huang, J. and Manning, B.D. (2009) A complex interplay between Akt, TSC2 and the two mTOR complexes. *Biochem. Soc. Trans.*, **37**, 217–222.
36. Sarbassov, D.D., Ali, S.M., Kim, D.H., Guertin, D.A., Latek, R.R., Erdjument-Bromage, H., Tempst, P. and Sabatini, D.M. (2004) Rictor, a novel binding partner of mTOR, defines a rapamycin-insensitive and raptor-independent pathway that regulates the cytoskeleton. *Curr. Biol.*, **14**, 1296–1302.
37. Schmidt, E.K., Clavarino, G., Ceppi, M. and Pierre, P. (2009) SUnSET, a nonradioactive method to monitor protein synthesis. *Nat. Methods*, **6**, 275–277.
38. Hua, Y., Sahashi, K., Hung, G., Rigo, F., Passini, M.A., Bennett, C.F. and Krainer, A.R. (2010) Antisense correction of SMN2 splicing in the CNS rescues necrosis in a type III SMA mouse model. *Genes Dev.*, **24**, 1634–1644.
39. Kelleher, R.J. 3rd. and Bear, M.F. (2008) The autistic neuron: troubled translation? *Cell*, **135**, 401–406.
40. Lehmann, S.M., Kruger, C., Park, B., Derkow, K., Rosenberger, K., Baumgart, J., Trimbuch, T., Eom, G., Hinz, M., Kaul, D. *et al.* (2012) An unconventional role for miRNA: let-7 activates Toll-like receptor 7 and causes neurodegeneration. *Nat. Neurosci.*, **15**, 827–835.
41. Packer, A.N., Xing, Y., Harper, S.Q., Jones, L. and Davidson, B.L. (2008) The bifunctional microRNA miR-9/miR-9* regulates REST and CoREST and is downregulated in Huntington's disease. *J. Neurosci.*, **28**, 14341–14346.
42. Gubitz, A.K., Feng, W. and Dreyfuss, G. (2004) The SMN complex. *Exp. Cell. Res.*, **296**, 51–56.
43. Pellizzoni, L. (2007) Chaperoning ribonucleoprotein biogenesis in health and disease. *EMBO Rep.*, **8**, 340–345.
44. Zou, T., Yang, X., Pan, D., Huang, J., Sahin, M. and Zhou, J. (2011) SMN deficiency reduces cellular ability to form stress granules, sensitizing cells to stress. *Cell. Mol. Neurobiol.*, **31**, 541–550.
45. Kedersha, N. and Anderson, P. (2007) Mammalian stress granules and processing bodies. *Methods Enzymol.*, **431**, 61–81.
46. Zhang, Y., Ueno, Y., Liu, X.S., Buller, B., Wang, X., Chopp, M. and Zhang, Z.G. (2013) The microRNA-17–92 cluster enhances axonal outgrowth in embryonic cortical neurons. *J. Neurosci.*, **33**, 6885–6894.
47. Kar, A.N., Macgibeny, M.A., Gervasi, N.M., Gioio, A.E. and Kaplan, B.B. (2013) Intra-axonal synthesis of eukaryotic translation initiation factors regulates local protein synthesis and axon growth in rat sympathetic neurons. *J. Neurosci.*, **33**, 7165–7174.
48. Zhu, H., Bhattacharyya, B.J., Lin, H. and Gomez, C.M. (2013) Skeletal muscle calpain acts through nitric oxide and neural miRNAs to regulate acetylcholine release in motor nerve terminals. *J. Neurosci.*, **33**, 7308–7324.

49. Dajas-Bailador, F., Bonev, B., Garcez, P., Stanley, P., Guillemot, F. and Papalopulu, N. (2012) microRNA-9 regulates axon extension and branching by targeting Map1b in mouse cortical neurons. *Nat. Neurosci.*, **15**, 697–699.
50. Ning, K., Drepper, C., Valori, C.F., Ahsan, M., Wyles, M., Higginbottom, A., Herrmann, T., Shaw, P., Azzouz, M. and Sendtner, M. (2010) PTEN depletion rescues axonal growth defect and improves survival in SMN-deficient motor neurons. *Hum. Mol. Genet.*, **19**, 3159–3168.
51. Bosch-Marce, M., Wee, C.D., Martinez, T.L., Lipkes, C.E., Choe, D.W., Kong, L., Van Meerbeke, J.P., Musaro, A. and Sumner, C.J. (2011) Increased IGF-1 in muscle modulates the phenotype of severe SMA mice. *Hum. Mol. Genet.*, **20**, 1844–1853.
52. Shababi, M., Glascock, J. and Lorson, C.L. (2011) Combination of SMN trans-splicing and a neurotrophic factor increases the life span and body mass in a severe model of spinal muscular atrophy. *Hum. Gene Ther*, **22**, 135–144.
53. Fernandez Alanis, E., Pinotti, M., Dal Mas, A., Balestra, D., Cavallari, N., Rogalska, M.E., Bernardi, F. and Pagani, F. (2012) An exon-specific U1 small nuclear RNA (snRNA) strategy to correct splicing defects. *Hum. Mol. Genet.*, **21**, 2389–2398.
54. Kye, M.J., Neveu, P., Lee, Y.S., Zhou, M., Steen, J.A., Sahin, M., Kosik, K.S. and Silva, A.J. (2011) NMDA mediated contextual conditioning changes miRNA expression. *PLoS One*, **6**, e24682.
55. Di Nardo, A., Kramvis, I., Cho, N., Sadowski, A., Meikle, L., Kwiatkowski, D.J. and Sahin, M. (2009) Tuberous sclerosis complex activity is required to control neuronal stress responses in an mTOR-dependent manner. *J. Neurosci.*, **29**, 5926–5937.
56. Elcheva, I., Goswami, S., Noubissi, F.K. and Spiegelman, V.S. (2009) CRD-BP protects the coding region of betaTrCP1 mRNA from miR-183-mediated degradation. *Mol. Cell*, **35**, 240–246.
57. Passini, M.A., Bu, J., Roskelley, E.M., Richards, A.M., Sardi, S.P., O'Riordan, C.R., Klinger, K.W., Shihabuddin, L.S. and Cheng, S.H. (2010) CNS-targeted gene therapy improves survival and motor function in a mouse model of spinal muscular atrophy. *J. Clin. Invest.*, **120**, 1253–1264.